Proceedings of the ASME 2016 35th International Conference on Ocean, Offshore and Arctic Engineering
OMAE2016
June 19-24, 2016, Busan, South Korea

OMAE2016-54420

BILGE KEEL INDUCED ROLL DAMPING OF AN FPSO WITH SPONSONS

Babak Ommani *
MARINTEK,
Trondheim, Norway
**babak.ommani@marintek.sintef.no*

Nuno Fonseca
MARINTEK,
Trondheim, Norway

Trygve Kristiansen
NTNU,
Trondheim, Norway

Christopher Hutchison
MARINTEK,
Trondheim, Norway

Hanne Bakksjø
Teekay Offshore Production,
Trondheim, Norway

ABSTRACT
The bilge keel induced roll damping of an FPSO with sponsons is investigated numerically and experimentally. The influence of the bilge keel size, on the roll damping is studied. Free decay tests of a three-dimensional ship model, for three different bilge keel sizes are used to determine roll damping coefficients. The dependency of the quadratic roll damping coefficient to the bilge keel height and the vertical location of the rotation center is studied using CFD. A Navier-Stokes solver based on the Finite Volume Method is adopted for solving the laminar flow of incompressible water around a section of the FPSO undergoing forced roll oscillations in two-dimensions. The free-surface condition is linearized by neglecting the nonlinear free-surface terms and the influence of viscous stresses in the free surface zone, while the body-boundary condition is exact. An averaged center of rotation is estimated by comparing the results of the numerical calculations and the free decay tests. The obtained two-dimensional damping coefficients are extrapolated to 3D by use of strip theory argumentations and compared with the experimental results. It is shown that this simplified approach can be used for evaluating the bilge keel induced roll damping with efficiency, considering unconventional ship shapes and free-surface proximity effects.

1 INTRODUCTION

An FPSO's roll motion is important from many aspects including stability, safety of personnel and operational limit of equipment. Therefore, during the design phase of an FPSO, and later to determine its window of operability, the behavior of the vessel in roll while experiencing different environmental conditions is always an important question.

Bilge keels are, by far, the most common tools for reducing the roll motion by introducing damping. The damping is the result of flow separation from the sharp edges of bilge keels. Despite the popularity of bilge keels, existing numerical methods, including the ones based on first principle modeling i.e. CFD, are not considered practical tools for prediction of bilge keel induced roll damping. This is mainly due to the complexity of the separated flow and its importance, which may lead to numerical modeling challenges and high computational cost. Hence other methods of estimation such as model testing and empirical methods are used in engineering and design.

Model testing is still the main practical tool for prediction of bilge keel loads and roll damping. A free decay test is the most common way to extract linear and quadratic roll damping coefficients (see for instance [1]). This method has the drawback of not properly considering the Keulegan-Carpenter (KC) number and frequency dependency. A more detailed description of roll damping properties of a vessel can be obtained by performing forced roll motions. Kristiansen et.al. [2] reported such a model test for an offshore service vessel. In this method a fixed center of rotation must be assumed. Assuming it even exists, determining an approximate center of rotation is a difficult task (see for instance [3]). Since the vessel is free to roll and sway, center of rotation is a less problematic issue in free decay tests.

Model tests can be used to assess the performance of bilge keels in reducing the roll response in irregular sea. Load measurements can be helpful in obtaining a better estimation of fatigue damages at the bilge keel root, which are known to be a problem for large FPSOs (for instance see [4]). However, model testing is usually expensive. In addition, performing experimental parameter studies to optimize a design can be impractical.

Application of potential flow theory codes is well established for predicting potential wave-radiation roll damping. However, viscous roll damping plays an important role in many realistic scenarios. For ships, strip theory is usually applied to calculate the roll damping of 3D bodies using the roll damping of 2D sections. Empirical formulas such as the Ikeda method [5], are usually used to estimate the nonlinear damping in roll due to bilge keels. However, a large uncertainty is generally associated with applying empirical methods to unconventional ship shapes. In particular, for estimating roll damping of large FPSOs with sponsons similar to the one studied in the present work.

A more recent approach involves application of CFD methods. As mentioned before, due to the complexity of the problem, this approach, even in two-dimensional form, carry a large computational cost (see for instance [6]). For example, in Volume of Fluid (VOF) method, capturing the free-surface with enough accuracy requires high resolution grids around the free-surface. Moreover, a nonlinear body-boundary condition is necessary for capturing the roll damping. Therefore, a method of grid deformation, over-lapping or sliding, must be used to capture the body-boundary motions accurately, which in turn increases the computational cost.

A hybrid approach, e.g. combination of potential and viscous flow methods, is another candidate for handling these types of complicated problems. This approach is rooted in simplifying complex flow problems by trying to capture the main contributing physics, instead of resolving all aspects of the problem from basic principles, e.g. Navier-Stokes equations using CFD. This approach requires a clear physical insight of what is important and what can be neglected in order to establish a valid numerical model. Analytical methods, experiments, and numerical parameter studies are among the main sources which can be helpful in providing this physical insight.

PVC, Potential Viscous Code, is a numerical code developed based on the hybrid approach (see [7]). Using PVC, it is possible to combine assumptions behind potential and viscous modeling to capture different aspects of the same problem. For instance, for a ship in forced roll motion, free-surface effects can be modeled using linear potential flow formulations and the flow separation from the bilge keel using Navier-Stokes equations.

An adaptation of the PVC code called PVC-2DRoll has been used here to model forced roll motions of a 2D section of an FPSO with sponsons and bilge keels. The hydrodynamic moment is decomposed and the linearized equivalent damping coefficient (b_{44}) is extracted. The linear part of the obtained 2D damping coefficients is neglected and the rest is extrapolated to 3D using a strip-theory type of approximation. The results are compared against the results of the vessel's free decay tests with three different bilge keel heights. The focus is on using the hybrid numerical method to estimate the variation of the quadratic roll damping by changing the bilge keel height, and validate the results with the experimental data.

2 MODEL TESTS

Free decay tests of an FPSO with sponsons were performed in the Ocean Basin at MARINTEK during April 2015. A photo of the model test set-up is provided in Fig. 1. The model scale was 1:60. All results given in this paper are in full scale, unless otherwise stated. The main particulars of the vessel are provided in Table 1. During the decay tests, the model mean position was maintained by a horizontal mooring system.

Fig. 1: Photo showing the vessel model in the MARINTEK's Ocean Basin.

Table 1. Main particulars of the ship model used in the decay tests in ballast condition. See Table 2 for more details.

Parameter	Model scale	Full scale
Length	4.283m	257.0m
Breadth	0.842m	50.5m
Draft	0.175 m	10.5m
Displacement	0.499 m^3	107 750 m^3
Bilge Keel Length	2.38m	142.8m
Bilge Keel Heights	0.017, 0.033, 0.042 m	1.5, 2.0, 2.5 m

The system consists of 4 very thin lines, in two pairs. One end of each line was connected to the model using a stiff clip and on the other end to the Ocean Basin sides by a soft linear spring. Two of the lines were connected to a single point at the model bow (see Fig. 1) and the others to a

similar point at the stern. The angular separation between lines was 90 degrees. The vertical position of the connection points was the same as the model's center of gravity.

The six degrees of freedom motions were measured by an optical-electronic system consisting of four light emitting diodes, strategically positioned on the model, and cameras located on the basin side. The decay tests were carried out for three bilge keel heights, namely: 1.5, 2.0 and 2.5 m. The bilge keel length and position was kept the same for the three groups of tests. The aim was to assess the influence of bilge keel size on the ship's roll damping. While one test only was performed for the 1.5 m bilge keel, ten tests were carried out for each of the other two bilge keel heights. The aim was to assess the experimental uncertainty of the estimated roll damping.

2.1 Model test data analysis

The decaying roll motion time signals were analyzed to identify the roll damping coefficient. A sample of a time series from a free decay test is shown in Fig. 2. The vessel is forced to roll for several periods, in this case about four periods, and released. The signals represent the roll motion and the sway and heave motion of the vessel's center of gravity. The first step is selecting the time window for analysis and identifying all roll peaks. The damping factor, or relative damping coefficient, is identified from the logarithmic decrement of two roll peaks:

$$\delta = \frac{1}{n} ln\left(\frac{x_i}{x_{i+n}}\right) \quad (1)$$

$$\zeta = \frac{1}{\sqrt{1 + (2\pi/\delta)^2}} \quad (2)$$

where δ is the logarithmic decrement, x_i and x_{i+n} are two roll peaks separated by n motion cycles, and ζ is the estimated damping factor, or relative damping. These formulae assume that the decaying roll motion can be represented by a one degree of freedom equation of motion (Eq. (5)).

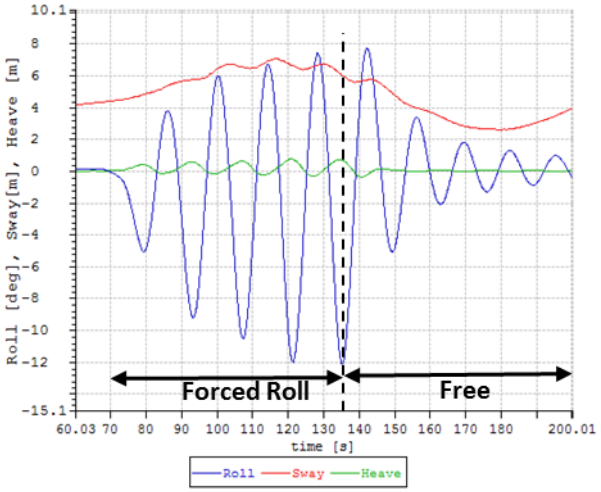

Fig. 2: Sample time series for a roll decay test. Note the coupling between roll and sway of the vessel's center of gravity.

The damping factor is estimated from consecutive roll peaks, which results on a number of estimates corresponding to each decay test. In Fig. 3, the roll damping factor estimates are presented for the three different bilge keel heights as a function of the roll mean amplitude from the total of 21 tests. Only one test belongs to the case with 1.5m bilge keel height, and the rest are equally divided between the 2.0 and 2.5 meters heights. The natural roll period of the vessel is estimated from the free decay tests to be around 12.9 seconds. It is of interest to note that the dispersion of results is relatively smaller for roll amplitudes above around 1.5 degrees, while a larger dispersion is observed for lower motion amplitudes. This is particularly true for the 2.0m bilge keel height cases. One concludes that the experimental uncertainty is smaller for the amplitudes above 1.5 degrees, and, the estimates are not reliable for small motion amplitudes. Fewer data points are available for angles larger than 4.0 degrees due to short transient time.

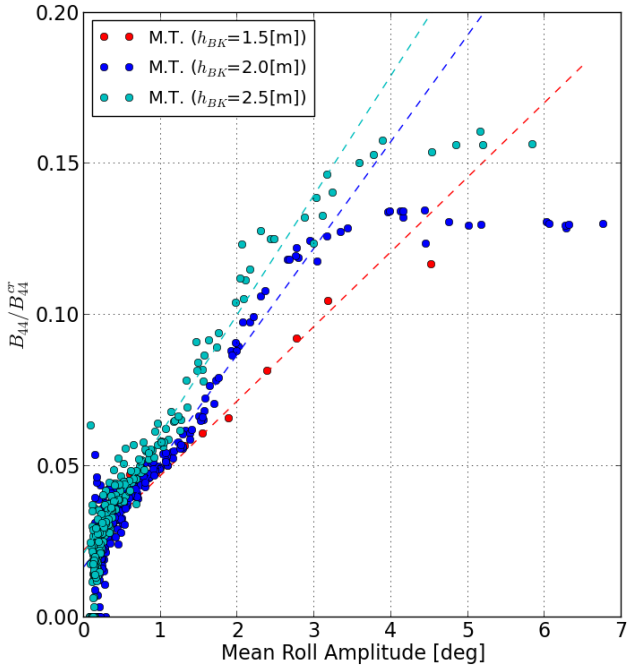

Fig. 3: Roll damping factor as a function of the mean roll amplitude estimated from decay tests. M.T.: Model Test, h_{BK}: bilge keel height.

In addition to the experimental data, Fig. 3 also shows three lines fitted to the model test data for each bilge keel height. These lines represent the quadratic roll damping model. Increase in the slope of the roll damping curve, i.e. quadratic damping, by increasing the bilge keel height is clear in Fig. 3. Moreover, the results for all three bilge keel heights deviates from the quadratic model by showing a drop in the slope for larger angles. This may be attributed to free surface effects which are discussed with more details in the following sections.

3 NUMERICAL SIMULATIONS

Numerical simulations for the mid-section of the FPSO are performed with *PVC-2DRoll,* which is a finite volume solver developed at MARINTEK based on OpenFOAM® package. The solution methodology is based on a hybrid method combining viscous and potential flow solvers [7]. It has been successfully applied and validated for moonpool [8,9] and ship roll [10,11] problems. In the latter context, the methodology has been further developed to account for large body motions.

Potential flow calculations for the complete vessel are performed using WAMIT® to obtain estimations of the vessel's critical damping. The 2D damping coefficients calculated by *PVC-2DRoll* are extrapolated to 3D by a strip theory type of assumption, and compared with the model test data.

3.1 Two-dimensional forced roll simulations

The problem of a 2D ship section undergoing forced roll oscillations about a fixed center of rotation (*C*) is considered. The mid-ship section of the vessel introduced in Sec. 2 is chosen for analysis. An inertial Earth-fixed coordinate system, *Oxyz*, is defined, where *x* points towards the aft of the vessel, *y* points towards starboard, and *z* is upward (Fig. 4). This is similar to the conventional seakeeping coordinate system, although, no forward speed is considered here.

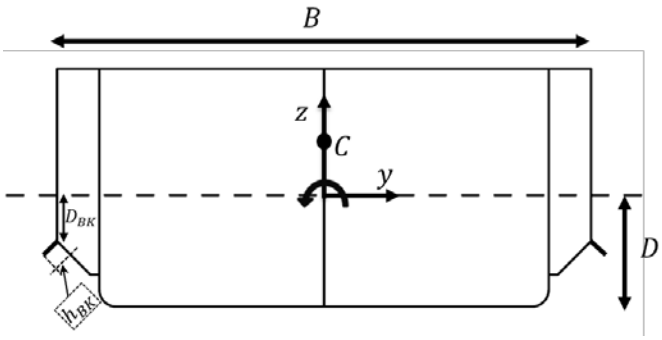

Fig. 4: Ship section schematic and coordinate system. *C*: center of rotation. See Table 2 for dimensions.

A hybrid modeling approach is adopted. Navier-Stokes equations in two dimensions are discretized using the Finite Volume Method (FVM), and solved for the water around the ship section. Laminar flow is assumed. This is justified due to presence of the bilge-keels which have sharp edges and fixes the flow separation point. The influence of bilge keels turbulent wake on the roll damping is neglected, assuming that the wake becomes easily turbulent and dissipates. Moreover, the effects of flow separation from the section's round bilge are neglected.

Fredriksen et al. [12] showed that the linearized body boundary condition is not sufficient for predicting the roll response of a two-dimensional body with a moonpool in waves. A significant difference in the predicted viscous roll damping was documented, depending on which of the linear or nonlinear body boundary conditions were used. This was also observed in the numerical study of forced roll motions of a ship section with bilge keels by Ommani et al. [10]. The reason is that the relative motions at the bilge keel tip are dominated by the body motions, and are therefore not sufficiently well modeled by linearized body-boundary condition. Therefore in the present study, the nonlinear body-boundary condition is satisfied by enforcing no flow through the instanteneous location of the body surface;

$$\vec{u} = \vec{u}_B \qquad on\ Body\ Surface \tag{3}$$

Here $\vec{u}$ is the water velocity vector and $\vec{u}_B$ is the body surface velocity vector. The free-surface boundary condition is linearized about the mean free-surface as shown in Eq.(4).

$$p = g\zeta \quad and \quad \frac{\partial \zeta}{\partial t} = u_3 \quad on\ Free\ Surface\ (z = 0) \tag{4}$$

Here *p* is the water pressure, ζ is the free-surface elevation, u_3 is the water velocity in the *z*-direction, g is the gravitational acceleration, and t denotes time. The linear free-surface condition is sufficient for this problem since the generated waves are of very small amplitudes and of linear nature.

To satisfy the nonlinear body boundary condition on a boundary fitted grid, a mesh deformation technique based on a solid body rotation (SBR) stress model available in OpenFOAM® is used to calculate cell deformations. A similar method has been successfully applied by Ommani and Faltinsen [13] to calculate forces on a deforming cross section in a 2D+t method.

Table 2: Dimensions of the FPSO's section with sponsons together with computation domain dimensions and number of cells; see Fig. 4 and Fig. 5

Section Beam (*B*)	50.5[m]
Section Draft (*D*)	10.5[m]
Section Characteristic Area ($A = BD$)	530.25[m^2]
Bilge Keel Draft (D_{BK})	4.3[m]
Bilge Keel Height (h_{BK})	1.5, 2.0, 2.5 [m]
COG Height (COG_z)	6.45 [m]
COR Height (COR_z) (Estimated)	~10.45 [m]
Domain Length / Ship Beam, (L_D/B)	100.0
Water Depth / Ship Beam, (H_D/B)	3.0
Approximate Number of Cells	~(30000 to 33000)

Since a linearized free surface condition is used, only the part of the domain filled with water is modeled and the part of the body surface below the free-surface is considered as body boundary (see Fig. 5). The underwater shape of the section at each time step is calculated using the imposed roll motion. The displacement of grid points on the body boundary is then imposed as a boundary condition in the mesh deformation boundary value problem.

The flow separation from the sharp edges of the bilge keels is assumed to be the dominant factor comparing to the boundary layer effects. Therefore, the mesh is not refined near the body boundary for capturing the boundary layer (Fig. 5). The mesh should be dense enough to capture pressure variations in the water due to radiated waves, i.e. one may use linear wave theory to estimate sufficient mesh density. This approach was demonstrated to be accurate and efficient in connection with moonpool resonance [8], and for roll wave radiation damping of ship shaped 2D sections [10].

Fig. 5 shows a sample of the generated mesh and a schematic view of the computational domain. The extent of the domain is chosen sufficiently large to avoid reflection of waves from end boundaries for the chosen duration of simulations. The main dimensions of the computational domain and the number of cells are given in Table 2 together with ship section dimensions. The number of cells for the generated grids is presented as an approximate value, since a series of different meshes were generated for different bilge-keel sizes.

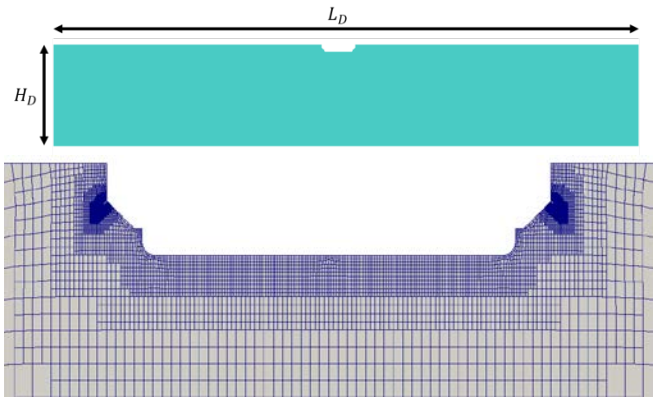

Fig. 5. Top: schematic of the computation domain, Bottom: A sample of the generated, body fitted mesh for the FPSO's section with sponsons and bilge keels at sponson's corner. The mesh is generated by Hexpress from Fine Marine® package.

The forces and moments acting on the body and bilge keels from the fluid are calculated by integrating the hydrodynamic pressure on the body surface. The obtained roll moment (F_4) is decomposed into the so-called added mass (a_{44}), damping (b_{44}) and linear restoring (c_{44}) terms as shown in Eq. (5) below.

$$a_{44}\ddot{\theta} + b_{44}\dot{\theta} + c_{44}\theta = F_4 \tag{5}$$

Here θ is the ship's roll angle and the dots represent time derivatives. The equivalent linearized damping coefficient in roll (b_{44}) is extracted by multiplying the obtained moment with angular velocity and integrating in time as shown in Eqs. (6) and (7) below,

$$\int_0^{nT} b_{44}\dot{\theta}\dot{\theta}dt = -\int_0^{nT} F_4\dot{\theta}dt \tag{6}$$

$$b_{44} = \frac{2\int_0^{nT} -F_4\dot{\theta}dt}{nT\left(\theta_a\omega\right)^2} \tag{7}$$

Here Θ_a is the amplitude, T is the period, and ω is the frequency of roll oscillations. Note that the nonlinear restoring term will not influence this analysis. The extracted damping coefficient in this way is still amplitude and frequency dependent. In order to minimize the transient solution, a linear ramp is adopted at the beginning of the imposed forced motion. The expression for oscillatory motion and its linear ramp is shown in Eq. (8) below.

$$\theta = \alpha\theta_a \sin\left(\frac{2\pi}{T}t\right), \qquad \alpha = \frac{t}{3T} \text{ for } t \le 3T \text{ and } \alpha = 1 \text{ for } t > 3T \tag{8}$$

The Euler method is used to march the solution forward in time. A fixed time-step is chosen for solving the problem. This is mainly due to the fact that having control over time-step improves the accuracy for extracting the damping coefficient. As discussed by Kristiansen et al. [2], capturing the correct phase between the roll moment and the roll velocity is essential in obtaining the correct damping coefficient. Here, the simulation time-step is chosen small enough in order to reduce possible errors due to phasing to a negligible level.

3.2 Potential flow calculations

A three-dimensional panel model of the vessel with bilge keel is prepared in MultiSurf® program (Fig. 6). The body surface is discretized with quadrilateral panels. The bilge keels are presented by dipole panels. WAMIT® is used for solving the potential flow radiation problem in roll and sway, and the obtained coefficients are transferred to the assumed center of rotation. The vessel's critical damping is estimated using the added mass and restoring coefficients from WAMIT®. The estimated natural frequency in roll is checked to be close to the obtained value from the free decay tests, i.e. 12.9 seconds (Sec. 2.1).

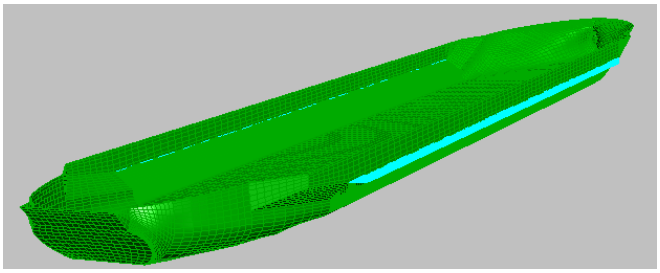

Fig. 6: Schematic view of the ship with bilge keel panel model for potential flow calculations using WAMIT®.

4 RESULTS AND DISCUSSIONS

The results of the two-dimensional viscous flow study, three-dimensional potential flow study, and the comparison

between experimental data and the numerical results are presented here.

4.1 Two-dimensional forced roll results

Fig. 7 shows the variation of the 2D section's roll damping coefficient with the vertical location of the rotation center. This parameter study helps quantify the dependency of the roll damping to the location of the rotation center. This dependency is particularly important since the location of the approximate center of rotation is not exactly known. The measured natural roll period ($T_n = 12.9$ seconds) is used as the forced rolling period.

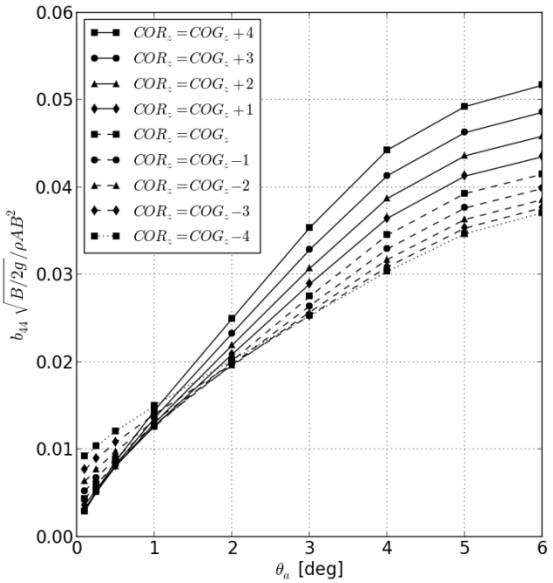

Fig. 7: Midsection roll damping coefficient as a function of roll amplitude for several vertical positions of the rotation center. Bilge keel height is 2[m]. See Table 2 for definition of symbols.

As expected, by moving the rotation center further up and away from the water-line, the slope of the roll damping curve as a function of the roll amplitude increases. This corresponds to larger quadratic damping, which is a result of higher flow velocities at the tip of the bilge keel.

The linear roll damping can be estimated by extrapolating the results in Fig. 7 to zero roll angle. Then, it becomes clear that moving the center of rotation up reduces the linear damping. The linear damping is mainly related to the wave radiation damping. Therefore, the vessel becomes a better wave maker when the center of rotation is moved further down and closer to the water line.

The dependency of the roll damping coefficient to the bilge keel height is shown in Fig. 8 for several vertical locations of the rotation center. The increase in the curves slope due to increase in the bilge keel height is evident. Furthermore, for all conditions, a drop in the slope of the roll damping coefficient is present for larger roll angles. It seems that the slope change starts at smaller angles when the bilge keel height is smaller. This may be attributed to the free surface effects on the vortices separated from the bilge keel tip. Then, it can be expected that larger bilge keels feel the free surface at higher angles, due to larger distance between bilge keel tip and the free surface. Furthermore, changing the bilge keel height changes the wave radiation which has influence on flow velocities at the bilge keel tip, and hence the quadratic damping. Additional studies are needed to confirm this point.

From Fig. 8, it is possible to see that changing the bilge keel height, slightly changes the linear roll damping as well. This suggests that, for this particular shape, the bilge keels affect the wave making ability of the body. Moreover, due to small distance between the bilge keel and free surface, wave radiation damping due to bilge keels are expected.

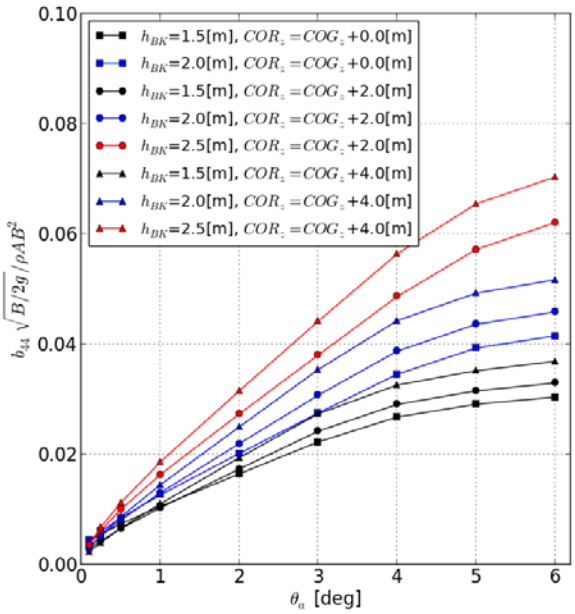

Fig. 8: Midsection roll damping coefficient as a function of roll amplitude for several bilge keel heights and vertical positions of the rotation center. See Table 2 for definition of symbols.

4.2 Three-dimensional potential flow results

Several parameter studies were performed to investigate the dependency of the wave radiation damping to the bilge keel height and the vertical location of the rotation center using WAMIT®. Fig. 9 shows the variation of the potential wave radiation damping in roll, non-dimensionalized by the critical roll damping, as a function of the vertical location of the rotation center with respect to the waterline, C_z. The results are for the studied FPSO with 2.0m bilge keel height. Similar to the results for the 2D calculations in Fig. 7, the wave radiation damping in roll, i.e. linear roll damping, decreases by increasing the height of the rotation center, and drops to less than one percent of the critical roll damping for the rotation center at the center of gravity.

Fig. 10 shows the relative potential damping variation with the bilge keel height. Again, similar to the conclusion presented for the 2D section in Fig. 8, the potential linear damping decreases by increasing the bilge keel height. This

means that the sum of the bilge keel's and the body's radiated waves reduces by increasing the height of bilge keel. This may be related to the phase difference between the two wave makers, i.e. the body and the bilge keels. Moreover, due to presence of sponsons and location of the bilge keels, they may change the effective beam to draft radio of the vessel which has strong effects on the vessel's wave making ability, and hence the linear roll damping.

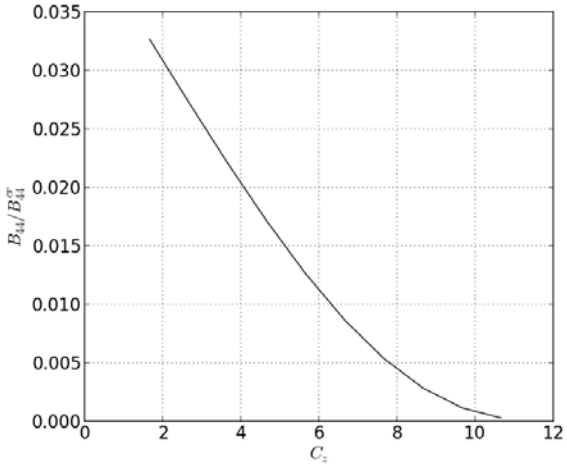

Fig. 9: Variation of the total nondimensional potential flow radiation damping as a function of the vertical location of the rotation center in meters for the FPSO with 2[m] bilge keel, and the roll natural period.

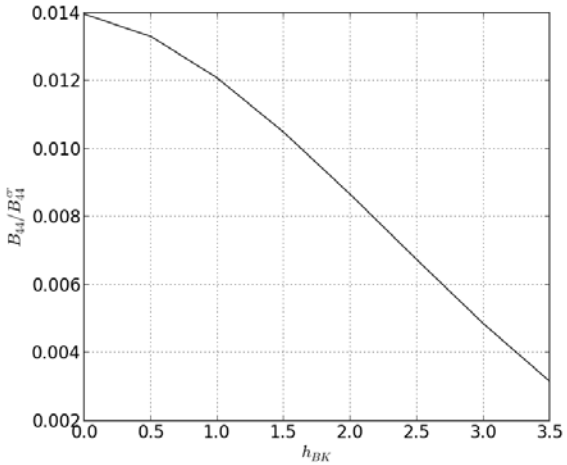

Fig. 10: Variation of the total nondimensional potential flow radiation damping as a function of the bilge keel height in meters for the center of rotation at COG, and the roll natural period.

4.3 Comparison with decay tests

The nonlinear part of the roll damping is extracted from the 2D calculations for the FPSO's mid-section, and extrapolated to 3D. In doing so, first the linear part of the roll damping, i.e. the extrapolated value for zero roll amplitude, has been subtracted from the results. This linear damping includes the section's wave radiation damping, and the bilge keel wave making effects. The remaining values are integrated along the vessel, assuming two-dimensional flow conditions and neglecting the end effects.

Only the length of the vessel equipped with bilge keel is considered (see Table 1). Meaning, the three-dimensional flow around the end of the bilge keels is also neglected. The shape of the vessel's cross section is almost constant along this length which justifies this simplified approach. It must be mentioned that other nonlinear effects, for instance due to eddy making and skin friction, are neglected here. However, since the main part of the nonlinear roll damping is due to bilge keels, their effects are expected to be of less importance. The vessel's linear damping is extracted from the free decay tests, by fitting a line to the results, and added to the obtained nonlinear damping values. Fig. 11, Fig. 12 and Fig. 13 show the obtained values for 1.5, 2.0, and 2.5 meters bilge keel height, respectively. The numerical results are presented for several locations of the rotation center. The locations are given relative to the vessel's center of gravity. In addition, the experimental values from free decay tests together with the fitted quadratic model, i.e. the fitted line, are presented.

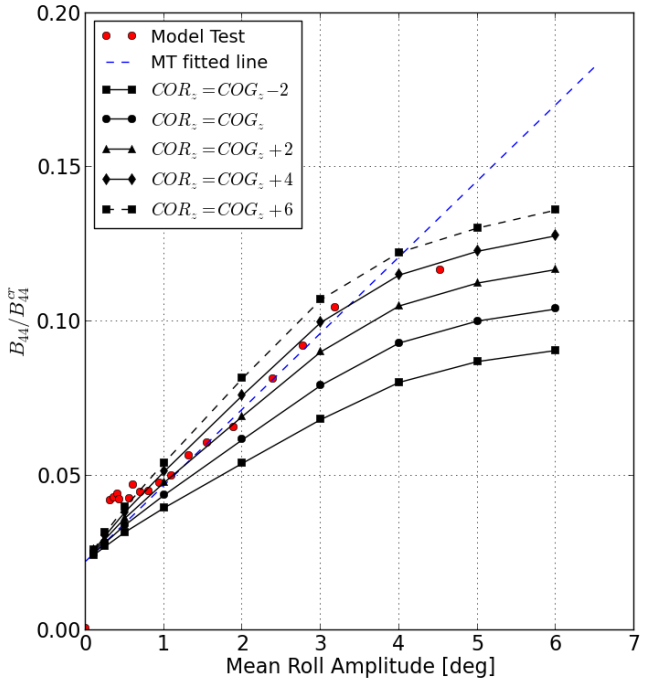

Fig. 11: Comparison of the present calculations and free decay model tests for the roll damping of the vessel with 1.5[m] bilge keel as a function of roll amplitude. See Table 2 for definition of symbols.

Assuming the existence of a fixed center of rotation for all roll amplitudes and bilge keel heights, the comparison of slopes suggests that it must be located around 4 meters above the center of gravity. For this to be true, the measurements of the center of gravity motions during free decay tests must show oscillatory sway motions with the roll natural frequency. Looking at the results in Fig. 2, it is possible to identify such characteristics in the motion. Assuming a single degree of freedom roll motion during free decay, it is possible to calculate an approximate value for the vertical distance between the rotation and gravity

center. The obtained value in this case is of a similar magnitude suggested by the calculations. However, neglecting the sway motion of the approximate rotation center may be questionable. Therefore, accurate estimation of the rotation center from the present experimental data is difficult.

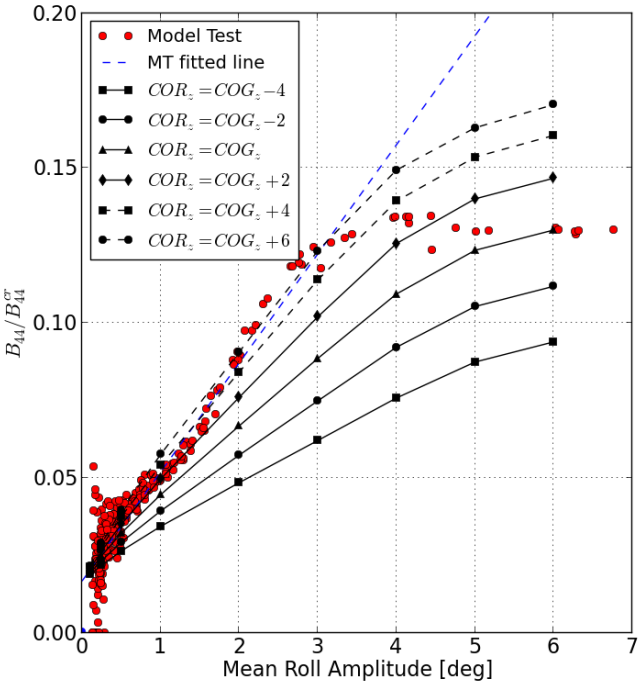

Fig. 12: Comparison of the present calculations and free decay model tests for the roll damping of the vessel with 2.0[m] bilge keel as a function of roll amplitude. See Table 2 for definition of symbols.

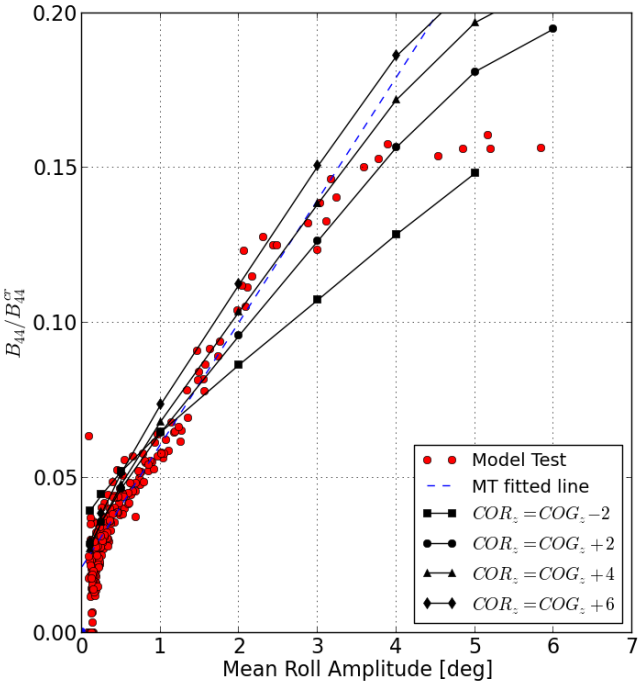

Fig. 13: Comparison of the present calculations and free decay model tests for the roll damping of the vessel with 2.5[m] bilge keel as a function of roll amplitude. See Table 2 for definition of symbols.

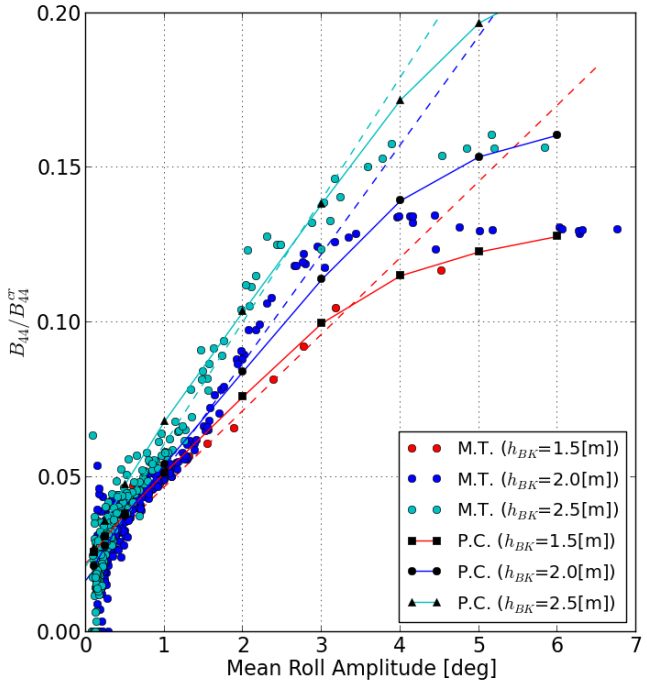

Fig. 14: Comparison of the present calculations and free decay model tests for the roll damping of the vessel as a function of roll amplitude. M.T.: Model Test, P.C.: Present Calculations. The rotation center is located 4.0m above the center of gravity. See Table 2 for definition of symbols.

Fig. 14 shows the comparison between the experimental roll damping values for the three different bilge keel heights, and the obtained values from the present method considering the rotation center to be 4.0 meters above the center of gravity. Generally a good agreement between the numerical results and experimental data is obtained. The increase in the roll damping by increasing the bilge keel height is captured by the numerical method (PVC) with reasonable accuracy. This means parameter studies for optimizing the bilge keel design, i.e. size, shape, and location, can be carried out by the proposed method. In particular, this may be important for ships with unconventional shapes similar to the FPSO studied here.

The deviation from the quadratic damping model suggests that the widely used empirical quadratic formulations, may over predict roll damping for the shapes such as the one studied here. Moreover, application of the quadratic model in time-domain simulation codes may result in under prediction of the roll response. Further studies are required to develop the present numerical method to a level that it can be used, together with time-domain simulators, to improve the roll response predictions.

5 CONCLUSIONS

The problem of predicting the roll damping coefficient of an FPSO with bilge keel and sponson was studied numerically and experimentally. The aim was to identify how the roll damping coefficient is changing with the bilge keel height.

Free decay tests were performed with the vessel's model at MARINTEK's Ocean Basin. Three different bilge keel heights were considered. The relative roll damping ratio was extracted from the tests and presented as a function of the mean roll amplitude. The quadratic roll damping model was fitted to the results, and its performance was discussed.

Two-dimensional numerical simulations for forced roll motion of the FPSO's mid-section were carried out using the hybrid code *PVC-2DRoll*. The estimated roll natural period was chosen as the forcing frequency. The rotation center and bilge keel was varied in order to study the dependency of the damping coefficients to these factors. It was shown that moving the center of rotation up and further away from the water line, increases the non-linear part of the roll damping while decreasing the linear part. The slope reduction of the roll damping as a function of the roll amplitude was addressed and attributed to the free surface effects.

Potential flow calculations were performed using WAMIT to obtain the roll critical damping, as well as linear wave radiation damping. Furthermore, it was shown that the roll damping due to wave radiation decreases by increasing the bilge keel height for the shape studied here.

The nonlinear part of the roll damping was extracted from the numerical calculations and integrated along the bilge keel length in order to obtain an estimation of the vessel's nonlinear roll damping. The resulted roll damping, after adding the linear component, was compared against free decay test results for three different bilge keel heights. The numerical parameter studies suggested that the approximate rotation center is located about 4.0m above the center of gravity. This was qualitatively confirmed by analyzing the sway motion during free decay tests. The uncertainties regarding the assumed center of rotation were addressed.

It was shown that the increase in the roll damping by increasing the bilge keel height was captured by the proposed numerical method with reasonable accuracy. This means that the proposed method can be used for parameter studies to optimize the bilge keel design, especially for ships with unconventional shapes. Deviations from the quadratic damping model were identified which were also captured by the numerical method, although in smaller magnitude. This deviation suggests that the widely used empirical quadratic formulations, may over predict the roll damping for the shapes such as the one studied here. Moreover, application of the quadratic model in time-domain simulation codes may result in under prediction of the roll response. Further studies are needed to develop the present numerical method to a level that it can be used, together with time-domain simulators, to improve the roll response predictions.

ACKNOWLEDGEMENTS

This research activity is partially funded by the Research Council of Norway through a Strategic Institute Program at MARINTEK. We acknowledge Teekay Offshore Production for the use of the model test data. In addition, the authors would like to thank Dr. Reza Firoozkoohi from MARINTEK for the helpful discussions.

6 REFERENCES

[1] O. M. Faltinsen, *Sea loads on ships and offshore structures*. Cambridge, UK: Cambridge University Press, 1990.

[2] T. Kristiansen, E. Ruth, R. Firoozkoohi, H. Borgen, and B. O. Berge, “Experimental and Numerical Investigation of Ship Roll Damping With and Without Bilge Keels,” in *33rd International Conference on Ocean, Offshore and Arctic Engineering*, San Francisco, California, USA, 2014, vol. 1B.

[3] A. C. Fernandes, P. Asgari, and A. R. W. Soares, “Asymmetric roll center of symmetric body in beam waves,” *Ocean Eng.*, vol. 112, pp. 66–75, Jan. 2016.

[4] R. van ’t Veer, “Time varying forces on FPSO bilge keels,” in *32nd International Conference on Ocean, Offshore and Arctic Engineering*, Nantes, France, 2013, vol. 5.

[5] Y. Ikeda, K. Komatsu, Y. Himeno, and N. Tanaka, “On roll damping force of ship -effects of hull surface pressure created by bilge keels-,” *J. Kansai Soc. Nav. Archit.*, vol. 165, no. 165, pp. 31–40, Jun. 1977.

[6] F. Jaouen, A. H. Koop, G. Vaz, and P. Crepier, “RANS predictions of roll viscous damping of ship hull sections,” in *V International Conference on Computational Methods in Marine Engineering*, Lisbon, Portugal, 2011.

[7] T. Kristiansen and O. M. Faltinsen, “Gap resonance analyzed by a new domain-decomposition method combining potential and viscous flow,” *Appl. Ocean Res.*, vol. 34, pp. 198–208, Jan. 2012.

[8] T. Kristiansen, T. Sauder, and R. Firoozkoohi, “Validation of a Hybrid Code Combining Potential and Viscous Flow With Application to 3D Moonpool,” 2013, p. V009T12A029.

[9] T. Kristiansen, B. Ommani, K. Berget, and R. Baarholm, “An Experimental and Numerical Investigation of a Box-Shaped Object in Moonpool; a Three-dimensional Study,” in *OMAE 2015*, 2015.

[10] B. Ommani, T. Kristiansen, and R. Firoozkoohi, “Non-linear roll damping, a parameter study,” in *The Twenty-fifth (2015) International Offshore and Polar Engineering Conference*, Kona, Big Island, Hawaii, USA, 2015.

[11] B. Ommani, T. Kristiansen, and O. M. Faltinsen, “Simplified CFD Modeling for Bilge Keel Force and Hull Pressure Distribution on a Rotating Cylinder,” *Submitted to Journal of Applied Ocean Research*, 2016.

[12] A. G. Fredriksen, T. Kristiansen, and O. M. Faltinsen, “Wave-induced response of a floating two-dimensional body with a moonpool,” *Philos. Transact. A Math. Phys. Eng. Sci.*, vol. 373, no. 2033, Jan. 2015.

[13] B. Ommani and O. M. Faltinsen, “Cross-flow transverse force and yaw moment on a semi-displacement vessel with forward speed and drift angle,” in *Proceedings of the 11th International Conference on Hydrodynamics (ICHD 2014)*, Singapore, 2014.